Proceedings of the 55th Israel Annual Conference
on Aerospace Sciences, Tel-Aviv & Haifa, Israel,
February 25-26, 2015

Transition to turbulence in plane Poiseuille flow

F. Roizner*, M. Karp and J. Cohen
Faculty of Aerospace Engineering, Technion - Israel Institute of Technology,
Haifa 32000, Israel

A transition to turbulence scenario in plane Poiseuille flow (PPF) initiated by Transient Growth (TG) associated with four streamwise elongated vortices is studied. Although the energy growth of this initial disturbance is less than that associated with two vortices, this combination is chosen because of its ability to generate relatively strong wall-normal inflection points in the velocity profile. It is shown that the TG stage is well approximated by using only the first five least stable even modes. Furthermore, the temporal modification of the base-flow includes the development of an inflection point in the wall-normal direction. Consequently, the modified base-flow becomes unstable with respect to three-dimensional infinitesimal secondary waves. The analytical predictions of key stages during this process are validated by direct numerical simulation (DNS). Moreover, the temporal evolution of the vortical structures through the process is well captured by the analytical model except for the last stage before breakdown to turbulence, where a packet of hairpin vortices is formed.

I. Introduction

Linear Stability Theory (LST) based on normal modes fails to predict instability in wall-bounded shear flows. In particular for PPF the critical *Re* number, based on centerline velocity and half channel height, is 5772 [1], whereas experimental investigations have shown that the transitional Reynolds number,i.e. the lowest Reynolds number for which turbulence can be sustained, is $Re \approx 1000$ [2, 3].

An alternative instability mechanism was first proposed by Ellingsen & Palm [4], who showed that for an inviscid fluid, the streamwise velocity component of a $3d$ disturbance with no streamwise variation grows linearly with time (unlike the exponential growth of normal modes). The inclusion of viscosity leads to the TG scenario in which the disturbance increases transiently and may reach a significant amplitude that can trigger nonlinear mechanisms before its eventual long-time exponential decay owing to viscous effects e.g. [5, 6].

It has been found by Gustavsson [7] for PPF that the initial structure in the linear case for which the kinetic energy amplifies the most is independent of the streamwise coordinate. Furthermore, two types of disturbances were found: symmetric and anti-symmetric ones; the latter achieving higher energy growth. The anti-symmetric disturbance consists of a counter-rotating vortex pair (CVP) whereas the symmetric one consists of two CVP's, one in the top half of the channel and the other in the bottom half (i.e. four vortices, see also [8]).

Transition scenarios in PPF initiated by two streamwise vortices (CVP) and a secondary disturbance, in the form of noise, have been investigated by Lundbladh *et al.* [9].

*froizner@tx.technion.ac.il

Accordingly, the CVP's modify the base-flow by forming streaks and generating inflection points. Stability analysis of the modified base-flow (PPF with the addition of a CVP) has been performed for the anti-symmetric disturbance by Reddy *et al.* [10]. They found that sinuous type instabilities, associated with spanwise inflection points, are more dominant than varicose instabilities, except at small vortex amplitudes. It should also be noted that the sinuous type instabilities play a key role in the destabilization of the flow during the self-sustaining process proposed by Waleffe [11].

The purpose of the present work is to investigate the transition scenario initiated by TG of four streamwise elongated vortices. This scenario has been much less studied in comparison with the TG initiated by a pair of vortices due to their greater TG potential. However, as demonstrated by Karp & Cohen [12] for Couette flow, maximal energy growth is not the essential parameter, rather it is the ability to generate inflection points in the base velocity profile. In order to validate our model, a comparison between the analytical and DNS results will be done.

II. Method

We consider a PPF in which the base-flow is parallel and is given by $U = 1 - y^2$, where U is the normalized streamwise base-flow velocity and $y \in [-1, 1]$ is the wall-normal direction, subjected to a primary $3d$ infinitesimal disturbance velocity. Assuming a normal mode solution, i.e. $[\tilde{u}, \tilde{v}, \tilde{w}, \tilde{p}] = [u, v, w, p](y) \exp(i(\alpha x + \beta z) - i\omega t)$, where $x \in (-\infty, \infty)$ and $z \in (-\infty, \infty)$ are the streamwise and spanwise directions, respectively, α and β are the streamwise and spanwise wavenumbers and ω is the angular frequency. As found by Gustavsson [7] the optimal TG is obtained for streamwise independent disturbances. Accordingly we consider a disturbance for which $\alpha = 0$. The associated Squire and Orr-Sommerfeld (OS) equations are:

$$[-i\omega - \frac{1}{Re}(D^2 - \beta^2)]\eta = -i\beta U' v, \tag{1}$$

$$[-i\omega - \frac{1}{Re}(D^2 - \beta^2)](D^2 - \beta^2)v = 0, \tag{2}$$

where $\eta(t, y, z)$ is the disturbance vertical vorticity and $D = \frac{d}{dy}$. These equations along with the boundary conditions that $v = 0$, $Dv = 0$ and $\eta = 0$ at $y = \pm 1$ complete the formulation of the linear problem in PPF. The analytical solution of this problem consists of two families of stable modes: symmetric and anti-symmetric ones with respect to $y = 0$.

Our purpose is to follow most of the transition process analytically. We therefore seek a minimal numbers of modes that can approximately follow the TG process, i.e. :

$$\mathbf{u}(t, y, z) = \sum_{n=1}^{N_{modes}} A_n \mathbf{u}_n(y) e^{i\beta z - i\omega_n t}, \tag{3}$$

where $\mathbf{u} = [u, v, w, p]$, t is the non-dimensional time and N_{modes} is the minimal number of modes required. In order to obtain maximal TG we demand the initial kinetic energy of the disturbance to be minimal. The amplitude of each mode is found analytically by satisfying $\frac{dE(0)}{dA_n} = 0$, where the kinetic energy density is defined as

$$E(t) = \frac{1}{2V} \int (|u|^2 + |v|^2 + |w|^2) dV, \tag{4}$$

where V is the volume of the domain. The gain of the energy is defined as the ratio between the energy at a given time, $E(t)$ and its initial value $E(0)$. This procedure results in two kinds of initial optimal disturbances: a single CVP and two CVP's when odd and even modes are used, respectively. As mentioned in the Introduction, we shall focus on the latter .

In spite of the fact that all modes composing the initial disturbance are stable, the combined disturbance grows for some time before its final decay due to viscous effects. This TG occurs due to the modes having different decay rates. As the disturbance grows it modifies the base-flow and in particular generates wall-normal and spanwise inflection points. Consequently, the modified base-flow becomes unstable with respect to $3d$ secondary infinitesimal disturbances which grow exponentially. On the other hand, the time scale associated with the TG is $O(Re)$. This separation of time scales allows us to perform a secondary stability analysis, assuming the modified base-flow is 'frozen' at a given time. Furthermore, from the analytical solution of the primary disturbance (TG), it can be observed that the wall-normal and spanwise velocities are $O(Re)$ smaller than the streamwise component. Therefore, for the purpose of the secondary stability analysis, we shall assume that the modified base-flow is parallel.

As our modified base-flow is periodic in the spanwise direction, we shall use Floquet theory. Accordingly, we consider an infinitesimal secondary disturbance of the form

$$[u_s, v_s, w_s, p_s] = e^{i\alpha x - i\omega_s t} \sum_{k=-M_k}^{M_k} [\tilde{u}_s, \tilde{v}_s, \tilde{w}_s, \tilde{p}_s]_k(y) e^{i\beta k z}, \tag{5}$$

where α is the streamwise wavenumber of the secondary disturbance and ω_s its temporal complex eigenvalue. Substituting eq. (5) into the linearized Navier-Stokes equations, for a base-flow of the form of $U = U(y, z; t)$, where t is a given time parameter for which the secondary stability analysis is performed. The resulted eigenvalue problem is solved numerically using MATLAB with 101 Chebyshev modes in the wall-normal direction. It has been found that $M_k = 5$ is sufficient to get converged eigenvalues.

Finally, in order to validate our method, the analytical TG solution is compared with DNS 'Channelflow' [13] results obtained for the same initial conditions.

III. Results

Fig.1 presents various linear TG scenarios for $Re = 3000$ and $\beta = 2$. The solid red curve corresponds to the optimal disturbance obtained numerically for many modes (e.g. [7]). The dashed blue curve corresponds to the optimal disturbance obtained numerically for only even modes which are the solutions of eq. 1 and 2. The black dashed-dot curve corresponds to the analytical TG using only five modes. It can be observed that about 85% of the optimal TG using many modes is captured using only five modes. The initial structure of the disturbance consists of a single CVP for the odd modes and a pair of CVPs for the even modes. Although the maximal growth of the optimal even TG is almost half of the growth of the optimal disturbance, we shall investigate its ability to generate inflection points and thereby lead to transition.

The initial cross-stream velocity field for the even case using only five modes is shown in Fig.2(A). In Fig.2(B) the modified base-flow at $t = 20$ is shown. The color represents the streamwise velocity. It can be seen that due to the action of the four vortices the flow is squeezed in the center generating inflection points in the flow field: the black dashed

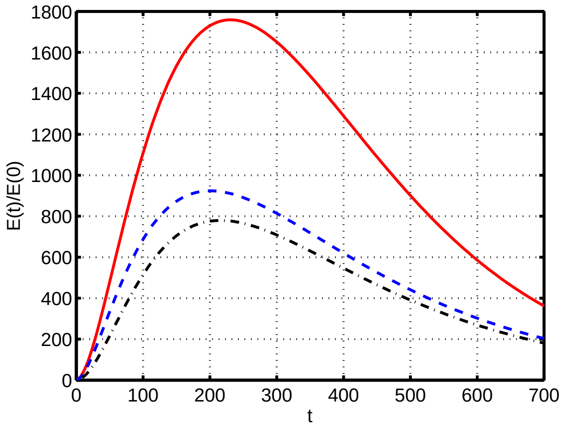

Figure 1. Energy growth obtained for streamwise independent modes, $Re = 3000$ and $\beta = 2$. The red solid curve corresponds to many odd modes, the blue dashed curve corresponds to many even modes and the black dashed-dot curve to five even modes.

contours are the location of wall-normal inflection points whereas the magenta dashed lines are the location of spanwise inflection points. In Figs (C) and (D) the corresponding wall-normal and spanwise distributions of the streamwise velocity are shown, respectively, with the inflection points indicated by the circles. It can be observed that there are four inflection points in the wall-normal direction, two near the walls and two near the center of the channel. The streamwise magnitude of the secondary disturbance is shown in Fig.3. It is clearly seen that the locations of the maximum strength correspond to the location of the two wall-normal inflection points which are closer to the center of the channel (see Fig.3).

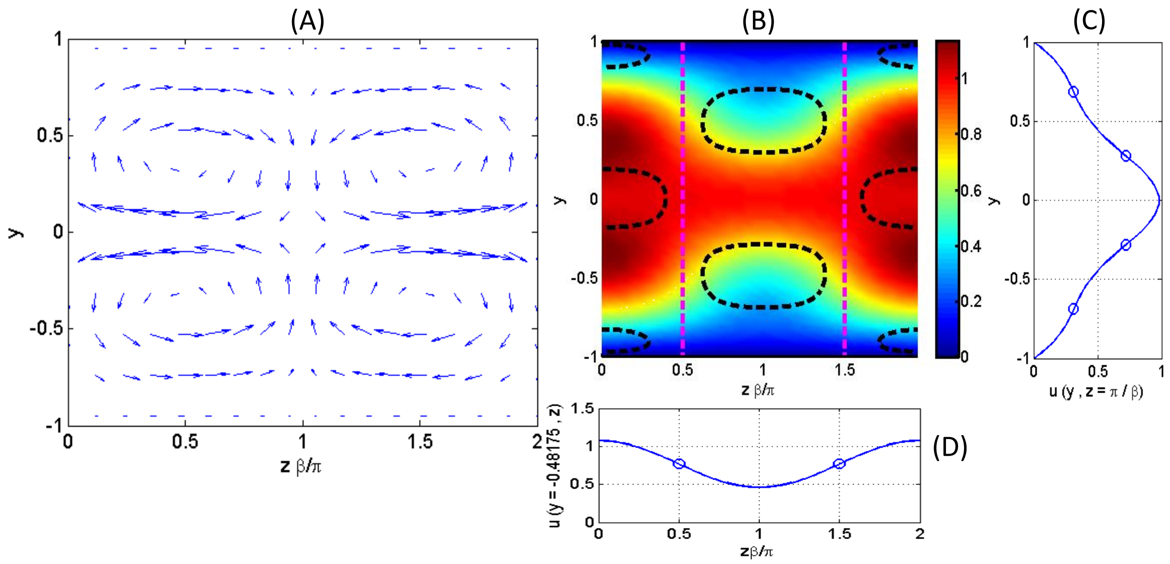

Figure 2. Even disturbance for $Re = 3000$ and $\beta = 2$. (A) The initial velocity field in the cross-section. (B) In color the modified base-flow at $t = 20$, the dashed black contours and magenta lines represent the inflection points in the wall-normal and spanwise directions, respectively. (C) The velocity profile at $z = \pi/\beta$. (D) The velocity profile at $y \approx 0.5$. The inflection points are encircled in (C) and (D).

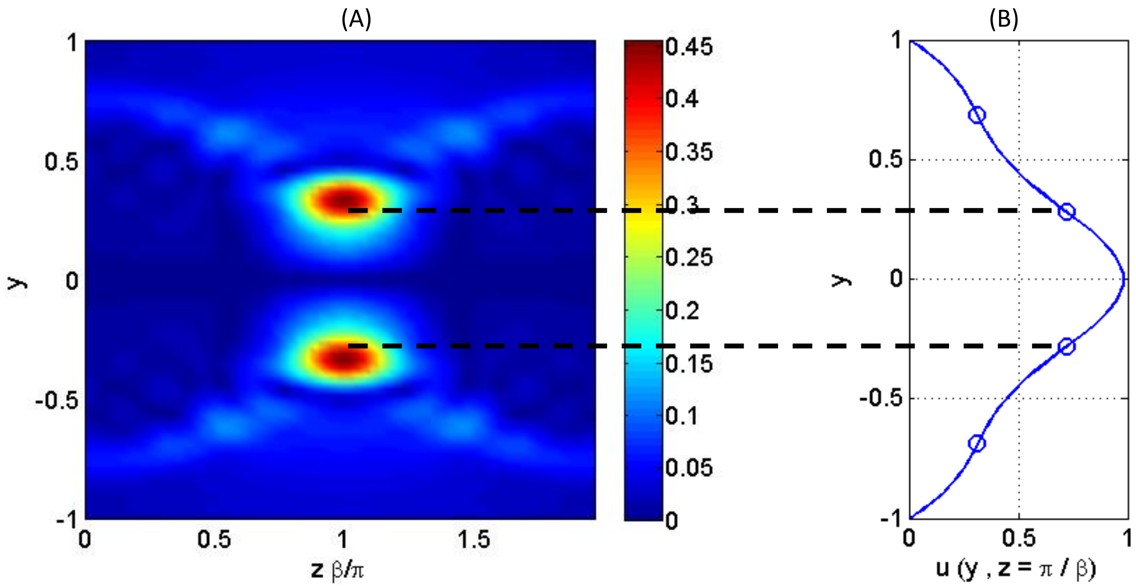

Figure 3. (A) The streamwise magnitude of the secondary disturbance for $Re = 3000$, $E(0) = 2 \times 10^{-4}$, $t = 20$, $\beta = 2$ and $\alpha = 3$. (B) The modified base-flow velocity profile at $z = \pi/\beta$.

Fig.4 shows the DNS results of the energy growth, initiated by the superposition of PPF together with the five TG modes and a calculated secondary disturbance. The broken blue curve corresponds to the initial disturbance associated with the initial disturbance composed by only the TG modes (the dashed-dot black curve in Fig.1). The initial energy of the disturbance is $E(0) = 2 \times 10^{-4}$. When a secondary mode obtained from the secondary stability analysis at $t = 20$ and $\alpha = 3$, with a relatively very small amplitude ($0.17\%E(0)$) is added, transition occurs rapidly (the red curve) preceded by a relatively long TG stage.

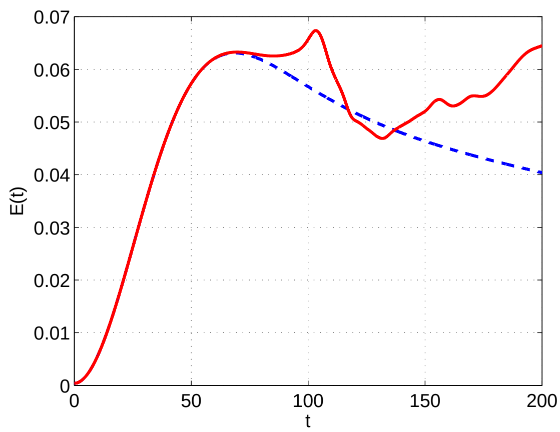

Figure 4. Energy growth obtained by DNS based on five even modes and a secondary disturbance obtained at $t = 30$ for $Re = 3000$ and $\beta = 2$. The unperturbed TG (i.e. without secondary disturbance) is given for reference (dashed line).

The temporal evolution of the vortical structures during the transition scenario associated with Fig.4 is presented in Fig.5 and Fig.6. Only the bottom half of the channel is plotted since the structures in the upper half are identical. To identify the vortical structure, Q , the second invariant of the velocity gradient tensor, is used. DNS and analytical results are shown respectively in the top and bottom rows of the figures. In order to obtain the vortical structures analytically, a constant growth of the secondary mode was assumed. Initially, the disturbance consists of four streamwise vortices (two in the top half of the channel and two in the bottom half) (Fig.5(A)). By $t = 30$ the structures experience a varicose instability (Fig.5(B)). At $t = 50$ (Fig.5(C)) streamwise-periodic spanwise vortical segments are formed above the wavy CVP. Each of these vortical structures expands and two streamwise 'sticks' are formed at its spanwise ends (Fig.6(A)). Consequently a packet of horseshoe vortices is formed (Fig.6(B)). The analytical vortical structures are plotted in Fig.5 (D),(E) and (F) and in Fig.6 (C) and (D). As can be seen the theoretical model is able to follow the DNS structures up to the stage where a packet of horseshoe vortices is formed, just before the final breakdown into turbulence.

IV. Concluding remarks

It is shown that five decaying modes are sufficient to approximately follow the transient growth scenario in PPF. This enables us to follow analytically the keys stages of the transition scenario. Comparison with similar results obtained for Couette flow [12] shows that while most of the energy growth in Couette flow is during the growth of the secondary disturbance, in PPF it occurs during the linear TG phase.

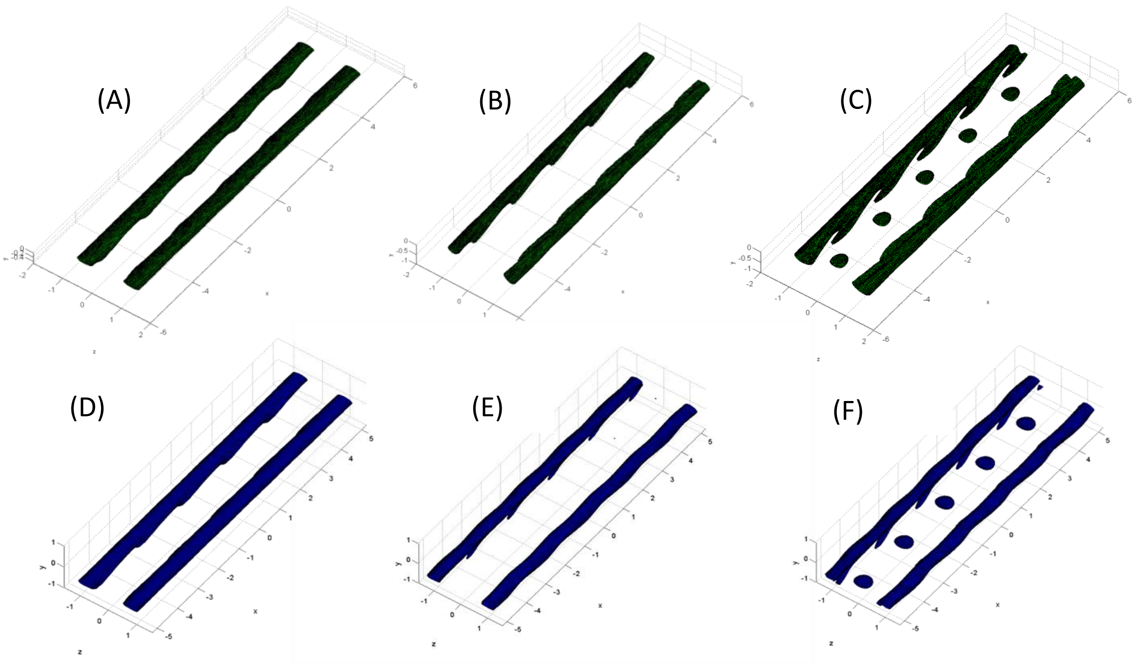

Figure 5. Vortex dynamics during early times in the transition as obtained from DNS (A), (B) and (C) and as obtained analytically in (D),(E) and (F). The structures are shown by iso-surfaces of the Q definition.

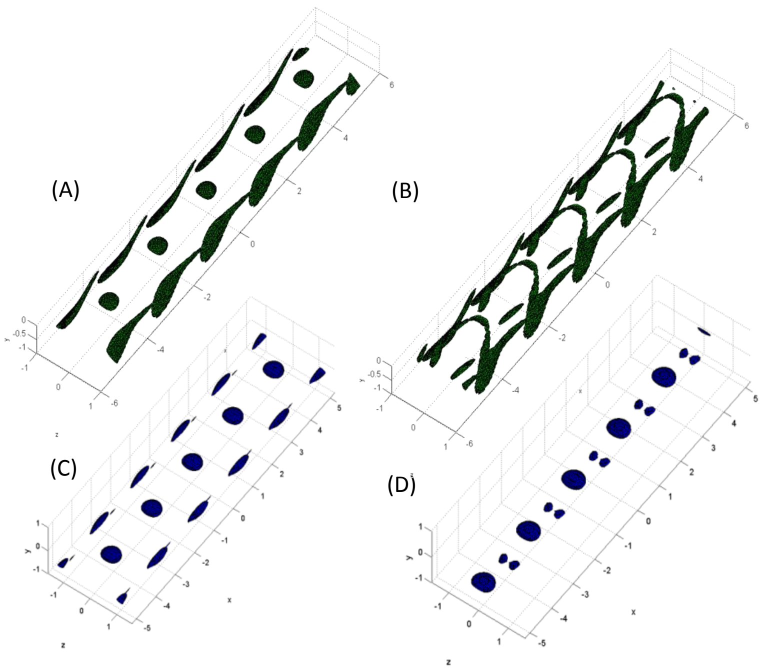

Figure 6. Vortex dynamics during later times in the transition as obtained from DNS (A) and (B) and as obtained analytically in (C) and (D). The structures are shown by iso-surfaces of the Q definition.

References

[1] Orszag, S., "Accurate solution of the Orr-Sommerfeld stability equation," *J. Fluid Mech.*, Vol. 50, 1971, pp. 689–703.

[2] Davies, S. and White, C., "An experimental study of the flow of water in pipes of rectangular section," *Proceedings of the Royal Society of London. Series A, Containing Papers of a Mathematical and Physical Character*, Vol. 119, 1928, pp. 92–107.

[3] Patel, V. and Head, M., "Some observations on skin friction and velocity profiles in fully developed pipe and channel flows," *J. Fluid Mech.*, Vol. 38, 1969, pp. 181–201.

[4] Ellingsen, T. and Palm, E., "Stability of linear flow," *Phys. Fluids*, Vol. 18, 1975, pp. 487–488.

[5] Reshotko, E. and Tumin, A., "Spatial theory of optimal disturbances in a circular pipe flow," *Phys. Fluids*, Vol. 13, 2001, pp. 991.

[6] Schmid, P., "Nonmodal stability theory," *Annu. Rev. Fluid Mech.*, Vol. 39, 2007, pp. 129–162.

[7] Gustavsson, L., "Energy growth of three-dimensional disturbances in plane Poiseuille flow," *J. Fluid Mech.*, Vol. 224, 1991, pp. 241–260.

[8] Butler, K. and Farrell, B., "Three-dimensional optimal perturbations in viscous shear flow," *Phys. Fluids A*, Vol. 4, 1992, pp. 1637–1650.

[9] Lundbladh, A., Henningson, D., and Reddy, S., "Threshold amplitudes for transition in channel flows," *Transition, turbulence and combustion*, 1994, pp. 309–318.

[10] Reddy, S., Schmid, P., Baggett, J., and Henningson, D., "On the stability of streamwise streaks and transition thresholds in plane channel flows," *J. Fluid Mech.*, Vol. 365, 1998, pp. 269–303.

[11] Waleffe, F., "On a self-sustaining process in shear flows," *Phys. Fluids*, Vol. 9, 1997, pp. 883.

[12] Karp, M. and Cohen, J., "Tracking stages of transition in Couette flow analytically," *J. Fluid Mech.*, Vol. 748, 2014, pp. 896–931.

[13] Gibson, J. F., "Channelflow: A spectral Navier-Stokes simulator in C++," Tech. rep., U. New Hampshire, 2012, `Channelflow.org`.